

Dirac neutrinos and N_{eff}

Xuheng Luo^{a,b}, Werner Rodejohann^b and Xun-Jie Xu^b

^a*University of Science and Technology of China, Hefei, Anhui 230026, China*

^b*Max-Planck-Institut für Kernphysik, Postfach 103980, D-69029 Heidelberg, Germany*

If neutrinos are Dirac particles the existence of light right-handed neutrinos ν_R is implied. Those would contribute to the effective number of relativistic neutrino species N_{eff} in the early Universe. With pure standard model interactions, the contribution is negligibly small. In the presence of new interactions, however, the contribution could be significantly enhanced. We consider the most general effective four-fermion interactions for neutrinos (scalar, pseudo-scalar, vector, axial-vector and tensor), and compute the contribution of right-handed neutrinos to N_{eff} . Taking the Planck 2018 measurement of N_{eff} , strong constraints on the effective four-fermion coupling are obtained, corresponding to interaction strengths of $10^{-5} \sim 10^{-3}$ in units of the Fermi constant. This translates in new physics scales of up to 43 TeV and higher. Future experiments such as CMB-S4 can probe or exclude the existence of effective 4-neutrino operators for Dirac neutrinos. Ways to avoid this conclusion are discussed.

I. INTRODUCTION

One of the most important questions in neutrino physics is whether neutrinos are Dirac or Majorana particles. The essential difference between the two cases is that a Dirac neutrino contains two more light degrees of freedom than a Majorana neutrino. These degrees of freedom correspond to light right-handed neutrinos (ν_R), which are absent in the Standard Model (SM) of particle physics. While theoretically the Majorana option is generally favored, every experimental measurement so far is in agreement with the Dirac hypothesis [1]. Indeed, many models and scenarios have been put forward that can forbid Majorana mass terms for the neutrinos and thus render neutrinos Dirac particles, see e.g. the review [2] for some references.

Even though the Dirac scenario implies the existence of ν_R , it is well known that those would not contribute significantly to the effective number of relativistic neutrino species N_{eff} in the early Universe, provided that neutrinos only interact as the SM predicts. With pure SM interactions, the smallness of neutrino Yukawa couplings means that ν_R would hardly couple to the SM thermal bath so that their energy density would be much lower than that of left-handed neutrinos ν_L — see e.g. the review [3].

However, since the existence of tiny neutrino masses is calling for new physics, it is reasonable to speculate that the interactions of neutrinos may also go beyond the SM. In general, if new neutrino interactions are present, then right-handed neutrinos could be thermalized and contribute significantly to N_{eff} . By requiring that the contribution does not exceed the current bound on N_{eff} , one can obtain very strong constraints on such new interactions. This is the content of our paper.

Already in Ref. [4], pure vector interactions of the form $G_V(\bar{\nu}\gamma^\mu\nu)(\bar{\nu}\gamma_\mu\nu)$ have been considered, and $G_V < 3 \times 10^{-3} G_F$, where G_F is the Fermi constant, has been derived by simply assuming that ν_R should have decoupled before the QCD phase transition ($T \approx 200$ MeV), which is roughly equivalent to $\Delta N_{\text{eff}} = \mathcal{O}(1)$. Nowadays, with precision data from CMB observations, ΔN_{eff} has been constrained more stringently. Currently the best measurement, $N_{\text{eff}} = 2.99 \pm 0.17$, comes from the Planck 2018 data [5, 6], which is consistent with the SM prediction $N_{\text{eff}}^{\text{SM}} = 3.045$ [7–9]. In the future, CMB Stage IV experiments (CMB-S4) are expected to reach a precision of $\Delta N_{\text{eff}} \sim 0.03$ [10, 11]. A very recent study [12] shows that with such precision, the cosmological constraints on some Dirac neutrino models such as unbroken (or adequately broken) $U(1)_{B-L}$ or neutrinophilic 2-Higgs

Doublet Models could exceed most laboratory constraints. Ref. [9] has considered the effect of the so-called Non-Standard Interactions (NSI) of the $V - A$ form, which have been extensively studied in the literature — see e.g. the reviews [13–16]. The paper concluded that NSI could reduce N_{eff} , depending on the flavor structure of the new interactions, down to 3.040 or enhance it to 3.059. In addition to these aforementioned scenarios, there has been a variety of other new physics scenarios proposed in the literature [17–23] that could affect N_{eff} .

In this work, we consider a set of effective four-fermion interactions of Dirac neutrinos with all possible Lorentz invariant forms, including scalar, pseudo-scalar, vector, axial-vector and tensor couplings, and study their effect on N_{eff} . Such *generalized neutrino interactions* have recently been discussed intensively [24–36]. Our study reveals that in this framework, N_{eff} could be significantly enhanced from new interactions involving ν_R , which therefore can be significantly constrained by current and future CMB experiments. Taking the constraint on N_{eff} from the Planck 2018 data, we derive upper bounds on the effective four-fermion couplings of the order $10^{-5} \sim 10^{-3} G_F$, depending on the interaction forms. This implies that new physics up to 43 TeV is probed. Future experiments such as CMB-S4 could fully exclude or probe this scenario, though there are ways to avoid this conclusion, which are discussed in this paper.

The paper is organized as follows: in Sec. II, we describe our set of new interactions, while in Sec. III we describe how those interactions enter the Boltzmann equation that describes the evolution of the right-handed neutrino density. This evolution, its effect on N_{eff} and the resulting limits on the new interactions are discussed in Sec. IV. Conclusions are presented in Sec. V, and various technical details are delegated to the Appendix.

II. GENERAL FOUR-FERMION INTERACTIONS

If neutrinos are Dirac particles and have new interactions beyond the SM, the right-handed components ν_R could have been in thermal equilibrium with the SM plasma. However, observation requires that they decouple from the SM plasma much earlier than the left-handed neutrinos ν_L . For example, the Planck 2018 data requires that in the presence of three ν_R , they should have decoupled at temperatures greater than $T > 600$ MeV [12]. This implies that if ν_R are in thermal equilibrium with ν_L , then they are also in thermal equilibrium with other SM particles, and vice versa. Therefore, considering only interactions between ν_R and ν_L can be very representative and also greatly simplifies the problem.

We formulate the new interactions of Dirac neutrinos as follows [25]:

$$\mathcal{L} \supset \frac{G_F}{\sqrt{2}} \sum_a \bar{\nu} \Gamma^a \nu [\bar{\nu} \Gamma^a (\epsilon_a + \tilde{\epsilon}_a i_a \gamma^5) \nu], \quad (1)$$

where the index $a = (S, P, V, A, T)$ denotes scalar, pseudo-scalar, vector, axial-vector and tensor interactions, i.e. the five possible combinations of Dirac matrices that could appear between two Dirac spinors:

$$\Gamma^a = \{I, i\gamma^5, \gamma^\mu, \gamma^\mu \gamma^5, \sigma^{\mu\nu} \equiv \frac{i}{2} [\gamma^\mu, \gamma^\nu]\}. \quad (2)$$

In Eq. (1), we have introduced $i_a = i$ for $a = S, P, T$ and $i_a = 1$ for $a = V, A$ so that ϵ_a and $\tilde{\epsilon}_a$ are real coefficients and Eq. (1) is self-conjugate¹.

¹ Otherwise an “h.c.” term should be added and the combined result would have the same form.

In principle, one could include flavor dependence in Eq. (1) by adding flavor indices to ν , $\bar{\nu}$, ϵ_a and $\tilde{\epsilon}_a$ — see e.g. [34]. With flavor dependence, ν_R of different flavors could have different decoupling temperatures. In this work, for simplicity, we assume the interactions are flavor universal and flavor diagonal, which means that the interaction in Eq. (1) exists for each generation of neutrinos with the same strength.

It is useful to express $\bar{\nu}\Gamma^a\nu$ in terms of chiral Dirac spinors $\nu_L = P_L\nu$ and $\nu_R = P_R\nu$, where $P_{L/R} \equiv (1 \mp \gamma^5)/2$:

$$\bar{\nu}\nu = \bar{\nu}_R\nu_L + \bar{\nu}_L\nu_R, \quad (3)$$

$$\bar{\nu}i\gamma^5\nu = -i\bar{\nu}_R\nu_L + i\bar{\nu}_L\nu_R, \quad (4)$$

$$\bar{\nu}\gamma^\mu\nu = \bar{\nu}_L\gamma^\mu\nu_L + \bar{\nu}_R\gamma^\mu\nu_R, \quad (5)$$

$$\bar{\nu}\gamma^\mu\gamma^5\nu = -\bar{\nu}_L\gamma^\mu\nu_L + \bar{\nu}_R\gamma^\mu\nu_R, \quad (6)$$

$$\bar{\nu}\sigma^{\mu\nu}\nu = \bar{\nu}_R\sigma^{\mu\nu}\nu_L + \bar{\nu}_L\sigma^{\mu\nu}\nu_R, \quad (7)$$

$$\bar{\nu}\sigma^{\mu\nu}i\gamma^5\nu = -i\bar{\nu}_R\sigma^{\mu\nu}\nu_L + i\bar{\nu}_L\sigma^{\mu\nu}\nu_R. \quad (8)$$

In the SM, neutrino interactions respect the $V - A$ form, which implies that only the combination $\bar{\nu}\gamma^\mu\nu - \bar{\nu}\gamma^\mu\gamma^5\nu = 2\bar{\nu}_L\gamma^\mu\nu_L$ is present, i.e. only left-handed neutrinos are involved.

Plugging Eqs. (3)-(8) into Eq. (1), we obtain several interaction terms linking left- and right-handed neutrinos:

$$\begin{aligned} \mathcal{L} \supset & G_S \bar{\nu}_L\nu_R\bar{\nu}_L\nu_R + G_S^* \bar{\nu}_R\nu_L\bar{\nu}_R\nu_L \\ & + \tilde{G}_S \bar{\nu}_L\nu_R\bar{\nu}_R\nu_L \\ & + G_V \bar{\nu}_L\gamma^\mu\nu_L\bar{\nu}_R\gamma_\mu\nu_R \\ & + G_T \bar{\nu}_L\sigma^{\mu\nu}\nu_R\bar{\nu}_L\sigma_{\mu\nu}\nu_R + G_T^* \bar{\nu}_R\sigma^{\mu\nu}\nu_L\bar{\nu}_R\sigma_{\mu\nu}\nu_L. \end{aligned} \quad (9)$$

Here we have defined new effective 4-fermion coefficients, namely

$$G_S = \frac{G_F}{\sqrt{2}} (\epsilon_S + i\tilde{\epsilon}_S - \epsilon_P - i\tilde{\epsilon}_P), \quad (10)$$

$$\tilde{G}_S = \sqrt{2}G_F (\epsilon_S + \epsilon_P), \quad (11)$$

$$G_V = \sqrt{2}G_F (\epsilon_V - \epsilon_A), \quad (12)$$

$$G_T = \frac{G_F}{\sqrt{2}} (\epsilon_T + i\tilde{\epsilon}_T). \quad (13)$$

In Eq. (9), we have neglected two terms $\bar{\nu}_L\gamma^\mu\nu_L\bar{\nu}_L\gamma_\mu\nu_L$ and $\bar{\nu}_R\gamma^\mu\nu_R\bar{\nu}_R\gamma_\mu\nu_R$, which cannot convert ν_R and ν_L into each other and would thus not contribute to generating right-handed neutrino energy densities in the early Universe.

Given the four-fermion operators in Eq. (9), there are five processes relevant to the evolution of the ν_R abundance ($\bar{\nu}_R$ has exactly the same thermal dynamics as ν_R) in the early Universe:

$$\nu_R + \nu_R \leftrightarrow \nu_L + \nu_L, \quad (14)$$

$$\nu_R + \bar{\nu}_R \leftrightarrow \nu_L + \bar{\nu}_L, \quad (15)$$

$$\nu_R + \nu_L \leftrightarrow \nu_R + \nu_L, \quad (16)$$

$$\nu_R + \bar{\nu}_L \leftrightarrow \nu_R + \bar{\nu}_L, \quad (17)$$

$$\nu_R + \bar{\nu}_L \leftrightarrow \bar{\nu}_R + \nu_L. \quad (18)$$

The scattering matrix elements of the above processes are computed in Appendix B. The result is summarized in Tab. I. Note that when one of the above processes (14)-(18) is present, right-handed

Table I. Processes that involve ν_R as initial or final states and the corresponding scattering matrix elements $|\mathcal{M}|^2$, assuming the presence of all terms in Eq. (9). Note that when used in phase space integrals containing identical particles, the matrix elements need to be multiplied by an additional symmetry factor S , see Eq. (22), which is not included in this table.

process	$ \mathcal{M} ^2$
$\nu_R(p_1) + \nu_R(p_2) \leftrightarrow \nu_L(p_3) + \nu_L(p_4)$	$16 G_S - 12G_T ^2(p_1 \cdot p_2)(p_3 \cdot p_4)$
$\nu_R(p_1) + \bar{\nu}_R(p_2) \leftrightarrow \nu_L(p_3) + \bar{\nu}_L(p_4)$	$4 \tilde{G}_S - 2G_V ^2(p_1 \cdot p_3)(p_2 \cdot p_4)$
$\nu_R(p_1) + \nu_L(p_2) \leftrightarrow \nu_R(p_3) + \nu_L(p_4)$	$4 \tilde{G}_S - 2G_V ^2(p_1 \cdot p_4)(p_3 \cdot p_2)$
$\nu_R(p_1) + \bar{\nu}_L(p_2) \leftrightarrow \nu_R(p_3) + \bar{\nu}_L(p_4)$	$4 \tilde{G}_S - 2G_V ^2(p_1 \cdot p_2)(p_3 \cdot p_4)$
$\nu_R(p_1) + \bar{\nu}_L(p_2) \leftrightarrow \bar{\nu}_R(p_3) + \nu_L(p_4)$	$16 G_S - 12G_T ^2(p_1 \cdot p_3)(p_2 \cdot p_4)$

neutrinos are automatically generated in the early Universe. For instance, in the presence of Eq. (16), which on its own would not generate right-handed neutrinos without an initial population, the process in Eq. (15) necessarily exists because the same couplings are involved. Hence, right-handed neutrinos are produced.

III. BOLTZMANN EQUATION

Recall that for a spatially homogeneous and isotropic Universe, we have

$$\dot{\rho}_{\text{tot}} + 3H(\rho_{\text{tot}} + P_{\text{tot}}) = 0, \quad (19)$$

where $H^2 = (\dot{a}/a)^2 = \frac{8\pi}{3m_{\text{Pl}}^2}\rho_{\text{tot}}$ is the Hubble parameter and ρ_{tot} and P_{tot} are the total energy density and pressure, respectively. Since we introduce ν_R to the SM, ρ_{tot} and P_{tot} can be decomposed as

$$\begin{aligned} \rho_{\text{tot}} &= \rho_{\text{SM}} + \rho_{\nu_R}, \\ P_{\text{tot}} &= P_{\text{SM}} + P_{\nu_R}, \end{aligned}$$

where the subscripts "SM" and " ν_R " denote the contributions from SM particles and from ν_R , respectively. The latter in general have a temperature T_{ν_R} that is different from the one of the SM particles T_{SM} , which we can consider to be the same for all SM particles, see the discussion after Eq. (28). Without any interactions between SM particles and ν_R , Eq. (19) could be applied to ρ_{SM} and ρ_{ν_R} individually, with the subscript "tot" replaced by "SM" and " ν_R ". However, in the presence of ν_R -SM interactions, there is energy transfer between the two components, which leads to the following evolution equations for ρ_{SM} and ρ_{ν_R} :

$$\dot{\rho}_{\text{SM}} + 3H(\rho_{\text{SM}} + P_{\text{SM}}) = -C_{\nu_R}^{(\rho)}, \quad (20)$$

$$\dot{\rho}_{\nu_R} + 3H(\rho_{\nu_R} + P_{\nu_R}) = C_{\nu_R}^{(\rho)}, \quad (21)$$

where $C_{\nu_R}^{(\rho)}$, known as a collision term, can be physically interpreted as the energy transfer rate from SM particles to ν_R . Taking the sum of Eqs. (20) and (21) yields again, as it should, Eq. (19). The explicit form of $C_{\nu_R}^{(\rho)}$ is derived from Boltzmann equations (see Appendix A), and given as follows:

$$\begin{aligned} C_{\nu_R}^{(\rho)} &= -N_{\nu_R} \int E_1 d\Pi_1 d\Pi_2 d\Pi_3 d\Pi_4 (2\pi)^4 \delta^4(p_1 + p_2 - p_3 - p_4) \\ &\quad \times S [|\mathcal{M}|_{1+2 \rightarrow 3+4}^2 f_1 f_2 (1-f_3)(1-f_4) \\ &\quad - |\mathcal{M}|_{3+4 \rightarrow 1+2}^2 f_3 f_4 (1-f_1)(1-f_2)], \end{aligned} \quad (22)$$

Table II. Collision terms $C_{\nu_R}^{(\rho)}$ computed for all the relevant processes including left- and right-handed neutrinos. In the third column, the $C_{\nu_R}^{(\rho)}$ are computed analytically from Maxwell-Boltzmann (MB) statistics. When used for neutrinos, the $C_{\nu_R}^{(\rho)}$ should be multiplied with Fermi-Dirac correction factors $1 - \delta_{\text{FD}}$ in the last column.

process	S	$C_{\nu_R}^{(\rho)}$ from MB statistics	$1 - \delta_{\text{FD}}$
$\nu_R(p_1) + \nu_R(p_2) \leftrightarrow \nu_L(p_3) + \nu_L(p_4)$	$\frac{2}{2!2!}$	$\frac{12}{\pi^5} G_S - 12G_T ^2 N_{\nu_R} (T_{\text{SM}}^9 - T_{\nu_R}^9)$	0.8840
$\nu_R(p_1) + \bar{\nu}_R(p_2) \leftrightarrow \nu_L(p_3) + \bar{\nu}_L(p_4)$	1	$\frac{2}{\pi^5} \tilde{G}_S - 2G_V ^2 N_{\nu_R} (T_{\text{SM}}^9 - T_{\nu_R}^9)$	0.8841
$\nu_R(p_1) + \nu_L(p_2) \leftrightarrow \nu_R(p_3) + \nu_L(p_4)$	1	$\frac{1}{2\pi^5} \tilde{G}_S - 2G_V ^2 N_{\nu_R} T_{\text{SM}}^4 T_{\nu_R}^4 (T_{\text{SM}} - T_{\nu_R})$	0.8518
$\nu_R(p_1) + \bar{\nu}_L(p_2) \leftrightarrow \nu_R(p_3) + \bar{\nu}_L(p_4)$	1	$\frac{3}{\pi^5} \tilde{G}_S - 2G_V ^2 N_{\nu_R} T_{\text{SM}}^4 T_{\nu_R}^4 (T_{\text{SM}} - T_{\nu_R})$	0.8249
$\nu_R(p_1) + \bar{\nu}_L(p_2) \leftrightarrow \bar{\nu}_R(p_3) + \nu_L(p_4)$	1	$\frac{6}{\pi^5} G_S - 12G_T ^2 N_{\nu_R} T_{\text{SM}}^4 T_{\nu_R}^4 (T_{\text{SM}} - T_{\nu_R})$	0.8118

$$d\Pi_i \equiv \frac{g_i}{(2\pi)^3} \frac{d^3 p_i}{2E_i}, \quad f_i \equiv \frac{1}{\exp\left(\frac{E_i}{T_i}\right) + 1}, \quad (i = 1, 2, 3, 4). \quad (23)$$

Here $1 + 2 \rightarrow 3 + 4$ represents the processes listed in Tab. I and $3 + 4 \rightarrow 1 + 2$ represents the inverse processes; g_i , E_i and T_i are the number of internal degrees of freedom, energy, and temperature of particle i . Without loss of generality, we always assign 1 to ν_R while 2, 3, and 4 may be assigned to any of ν_R , $\bar{\nu}_R$, ν_L , and $\bar{\nu}_L$, depending on the processes taken from Tab. I; S is a symmetry factor related to the number of identical particles in the initial/final states and N_{ν_R} is the number of right-handed neutrinos, both to be explained in detail later, see Eq. (25).

The collision term $C_{\nu_R}^{(\rho)}$ in Eq. (22) is a 12-dimensional integral, hence the numerical evaluation can be very time-consuming. Fortunately, by applying a technique developed in Refs. [37, 38]², we can drastically reduce it to a 3-dimensional integral. For massless particles obeying Maxwell-Boltzmann statistics, the 3-dimensional integral can be further integrated analytically, giving a purely analytical result. Neutrinos in our work can be treated as massless particles but they obey Fermi-Dirac statistics. Nevertheless, by expanding the Fermi-Dirac distributions in terms of $\exp(-E/T)$ with Maxwell-Boltzmann distributions as leading order approximation, one can obtain a good approximation [3]. A recent numerical study in Ref. [22] shows that the difference between Fermi-Dirac and Maxwell-Boltzmann statistics can be accounted for by multiplying the collision terms with a factor of $1 - \delta_{\text{FD}}$ with $\delta_{\text{FD}} = \mathcal{O}(0.1)$. In Appendix C, we use the technique of Ref. [38] to reduce the dimension of the integral and integrate the 3-dimensional integral analytically for Maxwell-Boltzmann statistics. The result is given in the third column of Tab. II. The Fermi-Dirac correction factor $1 - \delta_{\text{FD}}$ then can be obtained by solving the integral numerically, and comparing to the analytical Maxwell-Boltzmann result. We performed this in a way similar to that used in Ref. [22], and our results for the five relevant scattering processes are summarized in Tab. II. We have checked that when our code is applied to ν_L decoupling in standard cosmology (i.e., ν_L - e scattering), the Fermi-Dirac correction factors reported in Ref. [22] can be reproduced.

Eqs. (20) and (21) are the main expressions of this work, which allow to determine the evolution of ν_R energy density in the early Universe. Three comments are given as follows:

First of all, for f_i in Eq. (23), we have assumed that there is no spectral distortion of neutrino energy distributions when they decouple from the SM plasma. This is only true if the effective degrees of freedom of the SM are constant during the decoupling (for instantaneous decoupling there would be no spectral distortion). In reality, this never strictly holds but can be taken as a good approximation. The well-studied SM neutrino decoupling may help to understand the magnitude of such spectral distortions. The SM neutrinos ν_L decouple from the SM plasma at T

² For practical use, we refer the readers to Appendix A of Ref. [38] and Appendix D in Ref. [20].

around 1 or 2 MeV, followed by electron-positron annihilation at $T \sim 0.5$ MeV. Note that none of these processes is instantaneous. Hence the annihilation is expected to slightly heat up the tail of $f_{\nu_L}(E)$, which leads to a known spectral distortion of neutrinos. Numerical calculations find that the distortion is about [3]

$$\delta f_{\nu_L}(E)/f_{\nu_L}(E) \sim 3 \times 10^{-4} \frac{E}{T} \left(\frac{11}{4} \frac{E}{T} - 3 \right). \quad (24)$$

For $E \sim T$, Eq. (24) implies a 0.01% distortion. Therefore, in our study of ν_R decoupling, the spectral distortion should be negligible.

The second comment concerns the symmetry factor S . Here we prefer to include it not in $|\mathcal{M}|^2$, so that the matrix elements respect crossing symmetry which is used in our calculation — see Appendix B. In the absence of identical particles, $S = 1$. In general, when there are n identical particles in the initial or final states, S should be multiplied by a factor of $\frac{1}{n!}$. If it happens that the particle is the ψ in $C_\psi^{(\rho)}$ (in this case, ν_R) is among the identical particles, one needs to further multiply S by n .³ Therefore, taking $\nu_R + \nu_R \rightarrow \nu_L + \nu_L$ as an example, we have $S = \frac{1}{2!} \times \frac{1}{2!} \times 2 = 1/2$, while for $\nu_R + \bar{\nu}_L \rightarrow \bar{\nu}_R + \nu_L$, which is related to the former by crossing symmetry, we put $S = 1$.

The last comment is on the internal degrees of freedom and differences between ν and $\bar{\nu}$. In standard cosmology, ν_L and $\bar{\nu}_L$ are often treated as the same relativistic species with two internal degrees of freedom, i.e. $g_i = 2$ in Eq. (23). In this convention, ρ_{ν_L} stands for the total energy density of both ν_L and $\bar{\nu}_L$. In principle, one could adopt a similar approach for ν_R and $\bar{\nu}_R$. However, when using the results in Tab. I, one may notice that some operators (e.g., $G_S \bar{\nu}_L \nu_R \bar{\nu}_L \nu_R$) can produce $\nu_R + \bar{\nu}_L \leftrightarrow \bar{\nu}_R + \nu_L$, but not $\nu_R + \nu_L \leftrightarrow \nu_R + \nu_L$. A simple way to cope with such a difference is that we treat ν_L and $\bar{\nu}_L$ as two different species with the same temperature (physically they are different as they have opposite lepton numbers). Likewise, ν_R and $\bar{\nu}_R$ are also treated as two different species. This implies that we treat ν_L , $\bar{\nu}_L$, ν_R , and $\bar{\nu}_R$ as four different species. Each of them has only one internal degree of freedom, i.e., we take $g_i = 1$ in Eq. (23). In this approach, Eq. (21) would actually split into two equations for ν_R and $\bar{\nu}_R$, with independent energy densities (ρ_{ν_R} and $\rho_{\bar{\nu}_R}$), pressures (P_{ν_R} and $P_{\bar{\nu}_R}$), and collision terms ($C_{\nu_R}^{(\rho)}$ and $C_{\bar{\nu}_R}^{(\rho)}$), respectively. Since ν_R and $\bar{\nu}_R$ have the same temperature ($T_{\nu_R} = T_{\bar{\nu}_R}$), one would have $\rho_{\nu_R} = \rho_{\bar{\nu}_R}$, $P_{\nu_R} = P_{\bar{\nu}_R}$, and $C_{\nu_R}^{(\rho)} = C_{\bar{\nu}_R}^{(\rho)}$, which would allow us to recombine them. Therefore, even though we conceptually split them, we do not need to do so explicitly. We can simply take them as different species, then focus on ν_R to compute the phase space integral, and eventually multiply the result by the number of different species. In this way, it is also straightforward to include three generations of neutrinos ($N_\nu = 3$) in our analyses. In conclusion, for g_i in Eq. (23), ρ_{ν_R} and P_{ν_R} in Eq. (21), and N_{ν_R} in Eq. (22), we take

$$g_i = 1, \quad \rho_{\nu_R} = 2 \times N_\nu \times \frac{7}{8} \times \frac{\pi^2}{30} T_{\nu_R}^4, \quad P_{\nu_R} = 2 \times N_\nu \times \frac{7}{8} \times \frac{\pi^2}{90} T_{\nu_R}^4, \quad N_{\nu_R} = 2 \times N_\nu. \quad (25)$$

Here $\frac{7}{8} \times \frac{\pi^2}{30} T_{\nu_R}^4$ and $\frac{7}{8} \times \frac{\pi^2}{90} T_{\nu_R}^4$ are contributions from one fermionic degree of freedom — see Eqs. (A6) and (A8) for a brief review of the related thermodynamics. The SM energy density and pressure can be computed from

$$\rho_{\text{SM}} = \frac{\pi^2}{30} g_\star^{(\rho)} T_{\text{SM}}^4, \quad P_{\text{SM}} = \frac{\pi^2}{90} g_\star^{(P)} T_{\text{SM}}^4, \quad (26)$$

where $g_\star^{(\rho)}$ and $g_\star^{(P)}$ are effective degrees of freedom of the SM. The SM contains $3 \times 3 \times 4$ quarks, 3×2 charged leptons, 3 left-handed neutrinos, $8 + 3 + 1$ gauge bosons, and one Higgs doublet.

³ See also the discussion below Eq. (71) in Ref. [3].

Therefore, at a sufficiently high temperature ($T_{\text{SM}} \gg$ any SM particle mass), we have $g_{\star}^{(\rho)} = g_{\star}^{(P)} = (36 + 6 + 3) \times 2 \times 7/8 + 12 \times 2 + 4 = 106.75$. For lower temperatures, the calculations of $g_{\star}^{(\rho)}$ and $g_{\star}^{(P)}$ can be very involved. Note that, in general, $g_{\star}^{(\rho)} \neq g_{\star}^{(P)}$ and $dg_{\star}^{(\rho,P)}/dT_{\text{SM}} \neq 0$. We refer to Ref. [39] for the latest results of $g_{\star}^{(\rho)}$ and $g_{\star}^{(P)}$, which are used in our numerical calculations.

IV. EVOLUTION OF ν_R ABUNDANCE IN THE EARLY UNIVERSE

To understand the behavior of right-handed neutrinos in the presence of new interactions, we start with the ratio of Eqs. (20) and (21):

$$\frac{d\rho_{\nu_R}}{d\rho_{\text{SM}}} = \frac{3H(\rho_{\nu_R} + P_{\nu_R}) - C_{\nu_R}^{(\rho)}}{3H(\rho_{\text{SM}} + P_{\text{SM}}) + C_{\nu_R}^{(\rho)}}. \quad (27)$$

Since ρ_{ν_R} and ρ_{SM} are functions of T_{ν_R} and T_{SM} , respectively, we can replace $d\rho_{\nu_R} \rightarrow \frac{\partial\rho_{\nu_R}}{\partial T_{\nu_R}} dT_{\nu_R}$ and $d\rho_{\text{SM}} \rightarrow \frac{\partial\rho_{\text{SM}}}{\partial T_{\text{SM}}} dT_{\text{SM}}$ in Eq. (27), leading to:

$$\frac{dT_{\nu_R}}{dT_{\text{SM}}} = \frac{3H(\rho_{\nu_R} + P_{\nu_R}) - C_{\nu_R}^{(\rho)}}{3H(\rho_{\text{SM}} + P_{\text{SM}}) + C_{\nu_R}^{(\rho)}} \frac{\partial\rho_{\text{SM}}}{\partial T_{\text{SM}}} \left(\frac{\partial\rho_{\nu_R}}{\partial T_{\nu_R}} \right)^{-1}. \quad (28)$$

Note that all the quantities on the right-hand side of Eq. (28) are essentially functions of T_{ν_R} and T_{SM} . Regarding T_{ν_R} as a function of T_{SM} , the function $T_{\nu_R}(T_{\text{SM}})$ is fully determined by the differential equation (28).

We use Eq. (28) to compute the evolution of T_{ν_R} (starting with $T_{\nu_R} = T_{\text{SM}}$) down to a few MeV before ν_L decouple. After ν_L decouple, the SM plasma itself splits into two decoupled components: (i) a photon and electron-positron plasma with a temperature denoted as T_{γ} , and (ii) left-handed neutrinos⁴ with a temperature T_{ν_L} . In principle, we would need to split Eq. (20) into two equations to appropriately describe the evolution of the now two SM contributions. However, this is not necessary because at this stage, ν_R must have been completely decoupled otherwise their contributions to N_{eff} would obviously be too large. In other words, $C_{\nu_R}^{(\rho)}$ at this temperature is extremely small compared to the Hubble expansion term in Eq. (21), so we can safely turn it off. In this case Eq. (21) simply implies $d\rho_{\nu_R} + 4\rho_{\nu_R}d\ln a = 0$, or, in a more familiar form, $T_{\nu_R} \propto a^{-1}$. All free-streaming relativistic species have the same $T(a)$ dependence.

Under this approximation, the final temperature of ν_R can be determined by

$$\frac{T_{\nu_R,0}}{T_{\nu_R,10}} = \frac{a_0^{-1}}{a_{10}^{-1}} = \left(\frac{4}{11} \right)^{1/3} \frac{T_{\gamma,0}}{T_{\gamma,10}}, \quad (29)$$

where the subscript ‘‘0’’ denotes any time after electron-positron annihilation, and the subscript ‘‘10’’ denotes the time when $T_{\text{SM}} = 10$ MeV. The first identity in Eq. (29) follows from the aforementioned relation $T_{\nu_R} \propto a^{-1}$ and the second identity is the result of the expression $a_0^3 T_{\gamma,0}^3 = \frac{11}{4} a_{10}^3 T_{\gamma,10}^3$ in standard cosmology. It can be derived from entropy conservation: $g_{\star,10}^{(s)} T_{\gamma,10}^3 a_{10}^3 = (2T_{\gamma,0}^3 + 6 \times \frac{7}{8} T_{\nu_L,0}^3) a_0^3$, where $g_{\star,10}^{(s)} = 4 \times 7/8 + 3 \times 2 \times 7/8 + 2 = 10.75$ (4 from electrons, 3×2 from neutrinos, and 2 from photons) are the relativistic degrees of freedom of the SM at 10 MeV and $T_{\nu_L,0}/T_{\gamma,0} = (4/11)^{1/3}$ is the ratio of the final temperatures of left-handed neutrinos and photons.

⁴ Strictly speaking, the decoupling of ν_L is flavor dependent, which however does not affect our discussions and analyses below.

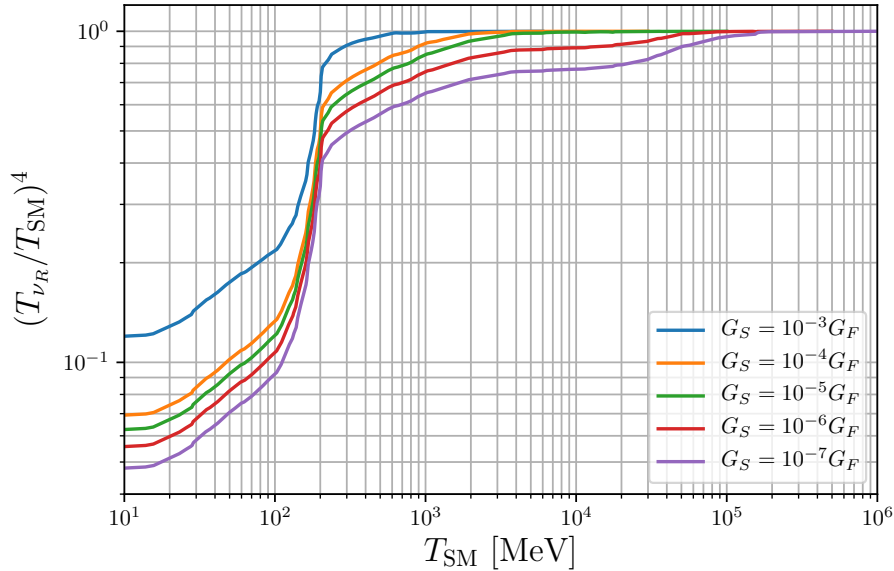


Figure 1. Temperature evolution of right-handed neutrinos for different new interactions, see Eq. (11).

Here we choose 10 MeV as a benchmark temperature because at this temperature all other SM particles can be safely neglected, and ν_L are still tightly coupled to electrons. These conditions allow us to compute $g_{*,10}^{(s)}$ by simply counting the numbers of fermions and bosons.

According to the definition of N_{eff} [7, 9], the contribution of ν_R to N_{eff} is given by:

$$\Delta N_{\text{eff}} = \frac{8}{7} \left(\frac{11}{4} \right)^{4/3} \frac{\rho_{\nu_R,0}}{\rho_{\gamma,0}}. \quad (30)$$

Using Eqs. (25), (26) and (29), we have:

$$\Delta N_{\text{eff}} = N_\nu \left(\frac{11}{4} \right)^{4/3} \frac{T_{\nu_R,0}^4}{T_{\gamma,0}^4} = N_\nu \left(\frac{T_{\nu_R,10}}{T_{\gamma,10}} \right)^4. \quad (31)$$

Therefore, to obtain ΔN_{eff} , we only need to solve Eq. (28) to obtain the temperature ratio at 10 MeV, which according to Eq. (31) immediately gives ΔN_{eff} .

With Eqs. (25) and (26) and the results in Tab. II, it is straightforward to solve Eq. (28). In Fig. 1, we present some solutions for G_S (see Eq. (10)) ranging from $10^{-3} G_F$ to $10^{-7} G_F$, assuming other interactions (\tilde{G}_S, G_V, G_T) are absent⁵. For other interactions, the curves are very similar. As we have just mentioned, we only solve the evolution equation down to 10 MeV, and the temperature ratio T_{ν_R}/T_γ can be directly used in Eq. (31) to obtain ΔN_{eff} . For example, the curve of $G_S = 10^{-4} G_F$ ends at 0.069, which implies that $\Delta N_{\text{eff}} = 3 \times 0.069 = 0.21$. For larger G_S , right-handed neutrinos decouple at lower temperatures, leading to higher values of T_{ν_R}/T_{SM} at the end, hence implying larger contributions to N_{eff} .

Let us support the numerical calculation with analytical considerations. Although the decoupling process is not instantaneous, one can nevertheless define a decoupling temperature T_{dec} from the

⁵ In Fig. 1, the initial value was set by $T_{\nu_R} = T_{\text{SM}}$. If it had been set to zero, the curves would quickly reach the SM temperature and the result is not changed.

condition

$$H \sim - \left. \frac{\partial \mathcal{C}_{\nu_R}^{(\rho)}}{\partial \rho_{\nu_R}} \right|_{T_{\nu_R}=T_{\text{SM}} \equiv T_{\text{dec}}} . \quad (32)$$

Using the results in Tab. II, we get:

$$H \sim T_{\text{dec}}^5 G_{\text{eff}}^2, \quad (33)$$

where G_{eff} is some combination of the coupling constants defined in Eq. (9), which can be estimated to be $G_{\text{eff}}^2 = \mathcal{O}(0.1)G_X^2$. To be precise, we obtain by analytically evaluating the right-hand side of Eq. (32) with the numerical values of $1 - \delta_{\text{FD}}$ in Tab. II that

$$G_{\text{eff}}^2 \equiv 0.28(G_S - 12G_T)^2 + 0.053(\tilde{G}_S - 2G_V)^2. \quad (34)$$

Combining Eq. (33) with Eqs. (25) and (26), we can solve for T_{dec} :

$$T_{\text{dec}} \sim 1.2 \times \frac{\left(g_*^{(\rho)} + 7N_\nu/4\right)^{1/6}}{\left(G_{\text{eff}}^2 m_{\text{pl}}\right)^{1/3}}. \quad (35)$$

Here $g_*^{(\rho)}$ is a temperature-dependent quantity (106.75 at $T_{\text{SM}} \gg 100$ GeV, and 10.75 at $T_{\text{SM}} = 10$ MeV) but the variation can be ignored due to the suppression by the exponent 1/6 (e.g., $10^{1/6} \approx 1.5$ and $100^{1/6} \approx 2.2$ are of the same order of magnitude). Taking $(g_*^{(\rho)} + 7N_\nu/4)^{1/6} \approx 2$, we can reformulate Eq. (35) as

$$T_{\text{dec}} \sim 2 \text{ MeV} \times \left(\frac{G_{\text{eff}}}{G_F}\right)^{-2/3}. \quad (36)$$

Taking for example $G_S \approx 10^{-7} G_F$, we have $G_{\text{eff}} \approx 5.3 \times 10^{-8} G_F$ and $T_{\text{dec}} \sim 1.4 \times 10^5$ MeV, which is qualitatively consistent with the purple curve presented in Fig. 1.

If the decoupling temperature is sufficiently high, the final temperature can be computed from entropy conservation. The entropy densities of ν_R and SM are (see Appendix A):

$$s_{\nu_R} = \frac{2\pi^2}{45} N_{\nu_R} \frac{7}{8} T_{\nu_R}^3, \quad s_{\text{SM}} = \frac{2\pi^2}{45} T_{\text{SM}}^3 g_*^{(s)}. \quad (37)$$

After decoupling, the entropy of ν_R and the entropy of the SM in a co-moving volume are conserved separately, i.e., $s_{\nu_R} a^3$ and $s_{\text{SM}} a^3$ remain constant. This gives

$$\begin{cases} T_{\text{dec}}^3 a_{\text{dec}}^3 = T_{\nu_R,10}^3 a_{10}^3 \\ T_{\text{dec}}^3 a_{\text{dec}}^3 g_{\star,\text{dec}}^{(s)} = T_{\text{SM},10}^3 a_{10}^3 g_{\star,10}^{(s)} \end{cases}, \quad (38)$$

where the subscripts "dec" and "10" denote the moments of ν_R decoupling and of $T_{\text{SM}} = 10$ MeV, respectively. The ratio of the two expressions in Eq. (38) results in:

$$\frac{T_{\nu_R,10}^3}{T_{\text{SM},10}^3} = \frac{g_{\star,10}^{(s)}}{g_{\star}^{(s)}(T_{\text{dec}})}. \quad (39)$$

Taking $g_{\star,10}^{(s)} = 4 \times 7/8 + 3 \times 2 \times 7/8 + 2 = 10.75$ (4 from electrons, 3×2 from neutrinos, 2 from photons) and $g_{\star,\text{dec}}^{(s)} = 106.75$ (the maximal value in the SM), we get

$$T_{\nu_R,10}/T_{\text{SM},10} = 0.465, \quad T_{\nu_R,10}^4/T_{\text{SM},10}^4 = 0.0468. \quad (40)$$

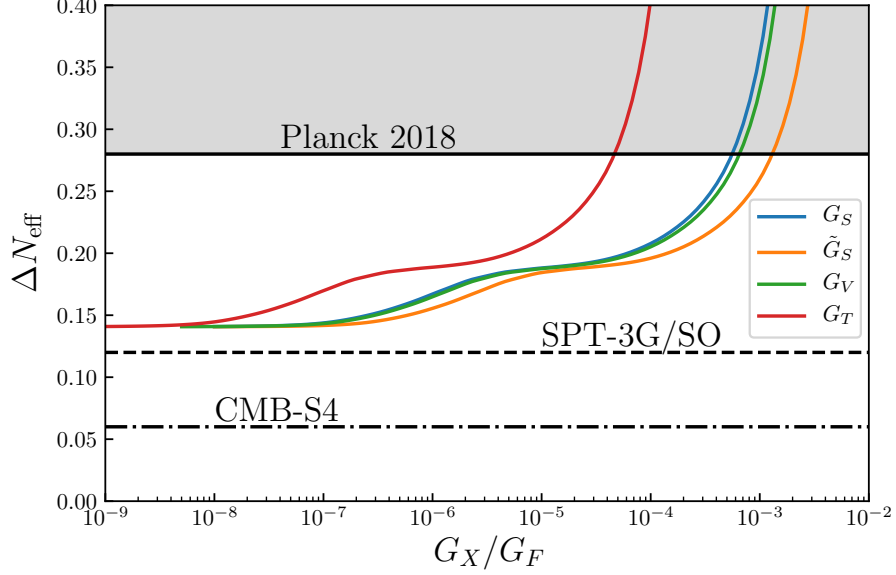


Figure 2. Contributions of ν_R to N_{eff} in the presence of G_S , \tilde{G}_S , G_V , G_T interactions defined in Eq. (9). The experimental bounds are presented at 2σ (95%) C.L.

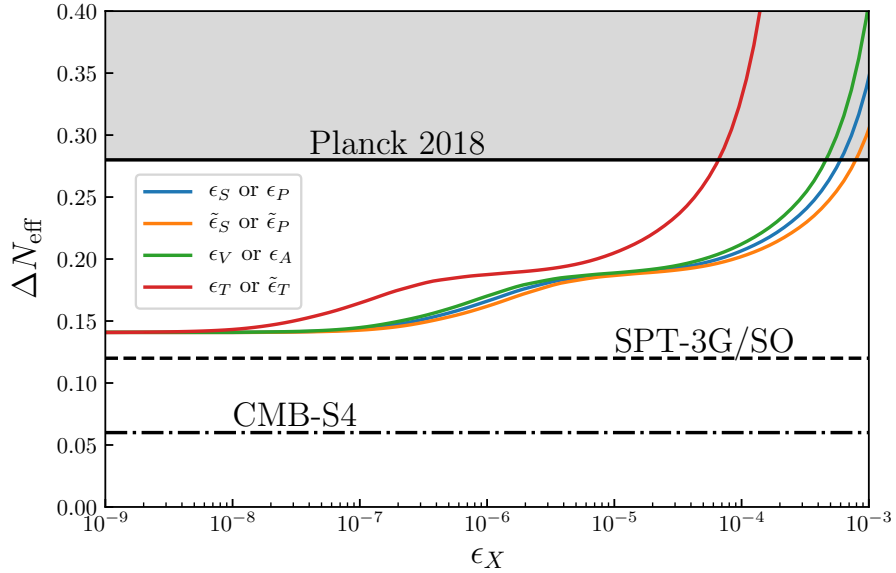


Figure 3. Same as Fig. 2 for the ϵ_X from Eq. (1).

This roughly matches the end of the lowest violet curve in Fig. 1. Therefore, if all three ν_R decouple at a temperature much higher than the electroweak scale, according to Eqs. (31) and (40), one would get $\Delta N_{\text{eff}} = 3 \times 0.0468 = 0.14$. Lower decoupling temperatures would lead to larger ΔN_{eff} , as demonstrated by the result of Ref. [12]: Planck 2018 data implies that three right-handed neutrinos should have decoupled at temperatures larger than 600 MeV.

In Fig. 2, we compute ΔN_{eff} for the four different types of interactions (G_S , \tilde{G}_S , G_V , G_T) and compare the results with current and future experimental limits on N_{eff} . Currently the Planck satellite [5, 6] has measured $N_{\text{eff}} = 2.99 \pm 0.17$ at 1σ confidence level (C.L.), which is so far

the strongest limit on N_{eff} . We put a 2σ bound (black solid curve) corresponding to $\Delta N_{\text{eff}} < 2.99 + 0.17 \times 2 - 3.045 = 0.285$. Future experiments such as the South Pole Telescope (SPT-3G) [40], the Simons Observatory (SO) [41], and CMB-S4 [10, 11] will significantly improve the measurement of N_{eff} . The SPT-3G is expected to be sensitive to ΔN_{eff} larger than 0.058 (1σ) and the SO sensitivity is very similar. So we take $\Delta N_{\text{eff}} < 0.12$ as a 2σ limit for both experiments. The CMB-S4 sensitivity is expected to reach 0.03 (1σ). So we take $\Delta N_{\text{eff}} < 0.06$ at 2σ C.L. for CMB-S4.

As shown in Fig. 2, the current limit on ΔN_{eff} from the Planck 2018 data implies at 2σ the following upper limits on the effective coupling constants in Eqs. (10)-(13):

$$G_S < 5.6 \times 10^{-4} G_F, \tilde{G}_S < 1.3 \times 10^{-3} G_F, G_V < 6.5 \times 10^{-4} G_F, G_T < 4.7 \times 10^{-5} G_F. \quad (41)$$

In Fig. 3 we show the result for the original parameters ϵ_X appearing in Eq. (1). The limits at 2σ C.L. are

$$\epsilon_{S,P} < 5.9 \times 10^{-4}, \tilde{\epsilon}_{S,P} < 7.9 \times 10^{-4}, \epsilon_{V,A} < 4.5 \times 10^{-4}, \epsilon_T, \tilde{\epsilon}_T < 6.5 \times 10^{-5}. \quad (42)$$

Alternatively, we can get a feeling for the energy scale that is probed by evaluating $\sqrt{1/G_X}$, which would correspond to m/g , where g is a new coupling and m the mass of a mediator particle. This gives:

$$\sqrt{1/G_S} > 12.4 \text{ TeV}, \sqrt{1/\tilde{G}_S} > 8.1 \text{ TeV}, \sqrt{1/G_V} > 11.4 \text{ TeV}, \sqrt{1/G_T} > 42.9 \text{ TeV}. \quad (43)$$

Note that for the values shown in Figs. 1, 2 and 3, it does not matter whether the initial temperature of the right-handed neutrinos is T_{SM} or zero. In the latter case T_{ν_R} approaches T_{SM} so quickly that no difference in the final result is visible.

Future limits from the SPT-3G/SO and CMB-S4 experiments would be lower than the minimal value ($\Delta N_{\text{eff}} = 0.14$) predicted in this framework, which implies that the scenario considered in this work could be fully excluded (up to some scenarios to be discussed below). On the other hand, if future measurements find a nonzero ΔN_{eff} larger than 0.14, Dirac neutrinos with BSM interactions would be one of the most well-motivated scenarios to explain the deviation.

Note, however, that in Fig. 2 one should not extrapolate the curves to arbitrarily small G_X . This would lead to the conclusion that even if $G_X \rightarrow 0$, ν_R would still contribute to N_{eff} with 0.14. Such an extrapolation relies on the assumptions that ν_R had been in thermal equilibrium with the SM, and that the number of effective degrees of freedom is indeed $g_*^{(\rho)} = 106.75$ for $T \gg 1$ TeV. Actually none of these assumptions may hold for very small G_X or very high T . Let us outline two scenarios which would change the lower bound of ΔN_{eff} .

(i) Consider that G_X is mediated by a heavy boson:

$$G_X = \frac{g^2}{m^2}, \quad (44)$$

where g is a new coupling and m is the mass of the new boson. For fixed m , $G_X \rightarrow 0$ would imply $g \rightarrow 0$. Let us examine Eq. (33) in this limit. If the ν_R had ever been in thermal equilibrium, then for decreasing G_X , their decoupling temperature would increase according to Eq. (36), and eventually would exceed m . Note that when $T \gg m$, the effective coupling would be $G_X \rightarrow g^2/T^2$, and hence the right-hand side of Eq. (33) would be proportional to $g^4 T$. On the left-hand side, the Hubble rate $H \propto T^2$ increases faster than $g^4 T$ as T further rises. Therefore, in this case,

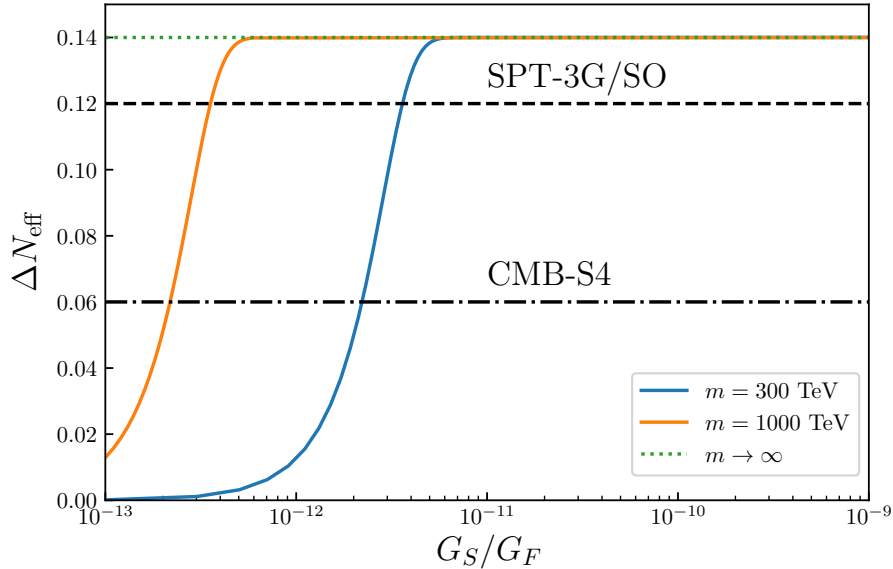


Figure 4. Illustration of possible modifications of the $\Delta N_{\text{eff}}-G_S$ relation when $G_S = g^2/m^2$ decreases while m is fixed at the given values.

Eq. (33) would have no solution with respect to T_{dec} , which implies that ν_R would never have been in thermal equilibrium with the SM.

If one numerically solves the Boltzmann equation, one can find that given an initial value $T_{\nu_R} = 0$, the temperature ratio T_{ν_R}/T_{SM} will eventually approach a constant (< 1), which is known as the freeze-in mechanism. Therefore, if $G_X \rightarrow 0$ is interpreted as $g \rightarrow 0$ with m fixed, ΔN_{eff} should vanish in this limit. In Fig. 4, we fix m at two values and solve, using $G_S = g^2/(m^2 + T^2)$, the Boltzmann equation with initial $T_{\nu_R} = 0$ to obtain the corresponding ΔN_{eff} for varying G_S . As can be seen from Fig. 4, for m fixed at finite values, ΔN_{eff} is suppressed for small G_S .

(ii) The lower bound $\Delta N_{\text{eff}} \geq 0.14$ depends significantly on the maximal value of $g_\star^{(s)}$. The maximal SM-value of 106.75, would be changed if there are more particles beyond the SM at higher energy scales. Note that from 2 MeV to 200 GeV, $g_\star^{(s)}$ increases by roughly a factor of 10. It is possible that from the electroweak scale up to the Planck scale, new physics substantially enhances $g_\star^{(s)}$ by another factor of 10 or more. According to Eqs. (31) and (39), taking $g_\star^{(s)}(T_{\text{dec}}) \approx 10^3$ for example, one would have $\Delta N_{\text{eff}} \approx 3 \times (10.75/1000)^{4/3} \approx 0.007$, which would be below the future CMB-S4 sensitivity.

As illustrated by the aforementioned two scenarios, the relic density of ν_R and ΔN_{eff} may be suppressed by new physics or by the model-dependent UV-completions of the new interactions. Here we refrain from further discussion and leave these possibilities to be studied in our future work. The bounds in Eq. (41) that we obtain on the new interactions can nevertheless be considered as robust.

V. CONCLUSION

Dirac neutrinos are a particularly interesting case of simple and straightforward physics that influences the effective number of relativistic degrees of freedom (N_{eff}) in the early Universe. Current and future data will put this possibility to the test.

We have considered here Dirac neutrinos with their most general effective interactions, as formulated in Eq. (1), and studied the constraints that Planck 2018 data puts on their strength. The new interactions would equilibrate the right-handed neutrinos and therefore lead to potentially large contributions to N_{eff} . Confronting this with Planck 2018 data leads to limits on the effective interaction strength of the order of 10^{-3} to 10^{-5} in units of the Fermi constant (see Figs. 2 and 3), or energy scales corresponding to up to 43 TeV and higher. Since the scenario of effective 4- ν operators predicts $\Delta N_{\text{eff}} \geq 0.14$, future experiments such as CMB-S4 which is expected to reach a sensitivity of $\Delta N_{\text{eff}} \sim 0.03$ can fully probe or exclude it. We commented on possibilities to avoid these conclusions.

ACKNOWLEDGMENTS

W.R. is supported by the DFG with grant RO 2516/7-1 in the Heisenberg program.

Appendix A: Thermodynamics

In this appendix, we briefly review some relevant aspects of equilibrium thermodynamics which are used in this work. Although most of the formulae can be found in textbooks (e.g., Kolb & Turner [42]), we would like to address some subtle issues via this brief review.

For particles in thermal equilibrium, their distribution f obeys the Bose-Einstein or Fermi-Dirac distributions:

$$f = \frac{1}{\exp\left(\frac{E-\mu}{T}\right) \mp 1}, \quad (\text{A1})$$

where “ \mp ” is “ $-$ ” for bosons and “ $+$ ” for fermions. The notations E , T , and μ are for the energy, temperature, and chemical potential of the particles, respectively. The definitions of energy density (ρ), number density (n), pressure (P), and entropy density (s) are

$$\rho \equiv \int E f(E) \frac{g}{(2\pi)^3} d^3p, \quad (\text{A2})$$

$$n \equiv \int f(E) \frac{g}{(2\pi)^3} d^3p, \quad (\text{A3})$$

$$P \equiv \int \frac{|\vec{p}|^2}{3E} f(E) \frac{g}{(2\pi)^3} d^3p, \quad (\text{A4})$$

$$s \equiv \frac{\rho + P}{T}. \quad (\text{A5})$$

Here g denotes the internal degrees of freedom. For massless or relativistic particles with negligible μ (typically this implies no particle-antiparticle asymmetry), all the above integrals can be evaluated analytically:

$$\rho = \frac{\pi^2}{30} g T^4 \times \begin{cases} 1 & (\text{boson}) \\ 7/8 & (\text{fermion}) \end{cases}, \quad (\text{A6})$$

$$n = \frac{\zeta(3)}{\pi^2} g T^3 \times \begin{cases} 1 & (\text{boson}) \\ 3/4 & (\text{fermion}) \end{cases}, \quad (\text{A7})$$

$$P = \rho/3, \quad (\text{A8})$$

$$s = \frac{2\pi^2}{45} g T^3 \times \begin{cases} 1 & (\text{boson}) \\ 7/8 & (\text{fermion}) \end{cases}. \quad (\text{A9})$$

Here $\zeta(3) \approx 1.202$ is a value of the Riemann zeta function. For multiple species in thermal equilibrium with each other, it is convenient to define effective degrees of freedom $g_\star^{(\rho)}$, $g_\star^{(n)}$, $g_\star^{(P)}$, and $g_\star^{(s)}$ via

$$\rho = \frac{\pi^2}{30} g_\star^{(\rho)} T^4, \quad n = \frac{\zeta(3)}{\pi^2} g_\star^{(n)} T^3, \quad P = \frac{\pi^2}{90} g_\star^{(P)} T^4, \quad s = \frac{2\pi^2}{45} g_\star^{(s)} T^3. \quad (\text{A10})$$

Here $g_\star^{(\rho)}$ is the most commonly used form of g_\star in the literature, typically appearing without the superscript (ρ) . For the SM, all these quantities have been comprehensively studied and computed in Ref. [39]. Note that Eqs. (A6) to (A9) hold only for relativistic particles while Eq. (A10) applies for both relativistic and non-relativistic particles. For particles with arbitrary masses, one can always use Eqs. (A2) to (A5) to compute ρ , n , P , and s , and then compute the corresponding $g_\star^{(\rho)}$, $g_\star^{(n)}$, $g_\star^{(P)}$ and $g_\star^{(s)}$ according to Eq. (A10).

When using Eq. (A10), it is important to note that $g_\star^{(\rho)}$, $g_\star^{(n)}$, $g_\star^{(P)}$, and $g_\star^{(s)}$ are also functions of T , which implies that in $d\rho/dT = 4\rho/T + \rho/g_\star^{(\rho)} dg_\star^{(\rho)}/dT$, the second term should not be ignored. It is also worth mentioning that since the energy density and pressure are related by⁶

$$dP = \frac{\rho + P}{T} dT, \quad (\text{A11})$$

one can derive an identity for $dg_\star^{(P)}/dT$,

$$\frac{dg_\star^{(P)}}{dT} = 3 \frac{g_\star^{(\rho)} - g_\star^{(P)}}{T}, \quad (\text{A12})$$

which is technically useful to determine $g_\star^{(P)}(T)$ and $g_\star^{(\rho)}(T)$ from each other if only one of them is given.

When several particle species in the early Universe interact with each other, their distributions are governed by the Boltzmann equation [3]:

$$\left[\frac{\partial}{\partial t} - H \vec{p} \cdot \nabla_{\vec{p}} \right] f_\psi(\vec{p}, t) = C_\psi^{(f)}. \quad (\text{A13})$$

Here ψ is a specific species of interest, and f_ψ is the distribution function of ψ , not necessarily in the form of Eq. (A1) if ψ is not in thermal equilibrium. The right-hand side is a collision term which for a given process $\psi + a + b + \dots \rightarrow i + j + \dots$ is computed by

$$\begin{aligned} C_\psi^{(f)} = & -\frac{1}{2E_\psi} \int d\Pi_a d\Pi_b \dots d\Pi_i d\Pi_j \dots (2\pi)^4 \delta^4(p_\psi + p_a + p_b + \dots - p_i - p_j - \dots) \\ & \times S \left[|\mathcal{M}|_{\psi+a+b+\dots \rightarrow i+j+\dots}^2 f_\psi f_a f_b \dots (1 \pm f_i)(1 \pm f_j) \dots \right. \\ & \left. - |\mathcal{M}|_{i+j+\dots \rightarrow \psi+a+b+\dots}^2 f_i f_j \dots (1 \pm f_\psi)(1 \pm f_a)(1 \pm f_b) \dots \right], \end{aligned} \quad (\text{A14})$$

with

$$d\Pi_x \equiv \frac{g_x}{(2\pi)^3} \frac{d^3 p_x}{2E_x}, \quad x \in \{\psi, a, b, \dots, i, j, \dots\}. \quad (\text{A15})$$

Here “ \pm ” takes “+” for bosons or “−” for fermions; S is a symmetry factor related to the number of identical particles in the initial/final states, and \mathcal{M} is the scattering amplitude of the process specified in its subscript.

⁶ See, e.g., Eq. (3.67) in Ref. [42].

Applying the $\vec{p} \cdot \nabla_{\vec{p}}$ operator in Eq. (A13) to the f in Eq. (A3) gives

$$\int \vec{p} \cdot \nabla_{\vec{p}} f \frac{g}{(2\pi)^3} d^3 p = \int [\nabla_{\vec{p}}(\vec{p} f) - f \nabla_{\vec{p}} \cdot \vec{p}] \frac{g}{(2\pi)^3} d^3 p = -3n, \quad (\text{A16})$$

where the $\nabla_{\vec{p}}(\vec{p} f)$ term vanishes because it is a total derivative (provided that $\vec{p} f \rightarrow 0$ if $p \rightarrow \infty$). Similarly, applying $\vec{p} \cdot \nabla_{\vec{p}}$ to the f in Eq. (A2), we have

$$\int E \vec{p} \cdot \nabla_{\vec{p}} f \frac{g}{(2\pi)^3} d^3 p = \int [\nabla_{\vec{p}}(E \vec{p} f) - f \nabla_{\vec{p}} \cdot (E \vec{p})] \frac{g}{(2\pi)^3} d^3 p = -3(\rho + P), \quad (\text{A17})$$

where we have used $\nabla_{\vec{p}} E = \vec{p}/E$. From Eqs. (A13), (A16) and (A17), we can obtain the following integrated Boltzmann equations:

$$\frac{dn_{\psi}}{dt} + 3Hn_{\psi} = C_{\psi}^{(n)}, \quad (\text{A18})$$

$$\frac{d\rho_{\psi}}{dt} + 3H(\rho + P) = C_{\psi}^{(\rho)}, \quad (\text{A19})$$

where

$$C_{\psi}^{(n)} \equiv \int C_{\psi}^{(f)} \frac{g_{\psi}}{(2\pi)^3} d^3 p_{\psi}, \quad (\text{A20})$$

$$C_{\psi}^{(\rho)} \equiv \int C_{\psi}^{(f)} \frac{E_{\psi} g_{\psi}}{(2\pi)^3} d^3 p_{\psi}. \quad (\text{A21})$$

Here one may wonder about the symmetry factor S in Eq. (A14). In the presence of identical particles, is the S factor in the collision term $C_{\psi}^{(f)}$ the same as the ones in $C_{\psi}^{(n)}$ and $C_{\psi}^{(\rho)}$? If among the particles a, b, \dots in Eq. (A14), n of them are identical to ψ and other particles are not identical, then the S factor should be $\frac{1}{n!}$. However, when $d^3 p_{\psi}$ further enters the phase space integral in Eqs. (A20) or (A21), the number of identical particles in the phase space integral increases by one to $n + 1$, hence leading to a factor of $\frac{1}{(n+1)!}$. On the other hand, when the n identical particles happen to be ψ , the process is n times more efficient in the conversion of particles or energy from ψ to other particles. Therefore, one should multiply the result by an additional factor of $1 + n$. Therefore, based on the number of identical particles in Eq. (A14), the S factor should be $\frac{1}{n!}$, while in Eqs. (A20) or (A21) it should be $\frac{n+1}{(n+1)!}$, which is the same as that in Eq. (A14).

Another noteworthy issue concerns a potential difference in using Eq. (A18) and (A19). Consider an elastic scattering process of ψ with particles of another species ψ' : $\psi + \psi' \rightarrow \psi + \psi'$, which eliminates one ψ and produces another ψ simultaneously. The corresponding $C_{\psi}^{(n)}$ vanishes but $C_{\psi}^{(\rho)} \neq 0$. Although this process does not contribute to $\frac{dn_{\psi}}{dt}$ directly, it leads to energy conversion from ψ' to ψ , or vice versa. If each species keeps thermal equilibrium internally and $T_{\psi} < T_{\psi'}$, then the energy injected to ψ via this process will increase ρ_{ψ} and T_{ψ} . Consequently, n_{ψ} has to be increased if ψ is relativistic and the internal thermal equilibrium of ψ is maintained. This is usually caused by self-interactions of ψ which could lead to processes such as $\psi + \bar{\psi} \rightarrow 2\psi + 2\bar{\psi}$. Therefore, if ψ keeps internal equilibrium via self-interactions, the collision term in Eq. (A18) has to take into account such processes, while in Eq. (A19) they can be ignored due to energy conservation.

Appendix B: Calculation of $|\mathcal{M}|^2$

In this appendix, we present the details of computing $|\mathcal{M}|^2$ for the processes listed in Tab. III.

Let us first start with the process

$$\nu_R(p_1) + \bar{\nu}_L(p_2) \rightarrow \bar{\nu}_R(p_3) + \nu_L(p_4). \quad (\text{B1})$$

Given the interactions in Eq. (9), only G_S and G_T can lead to this process. In the presence of G_S and G_T , the scattering amplitude reads:

$$i\mathcal{M}^{s_1 s_2 s_3 s_4} = \sum_{a=S,T} \{2(iG_a) [\bar{v}_2^{s_2}(p_2) P_R \Gamma^a P_R u_1^{s_1}(p_1)] [\bar{u}_4^{s_4}(p_4) P_R \Gamma^a P_R v_3^{s_3}(p_3)] - 2(iG_a) [\bar{u}_4^{s_4}(p_4) P_R \Gamma^a P_R u_1^{s_1}(p_1)] [\bar{v}_2^{s_2}(p_2) P_R \Gamma^a P_R v_3^{s_3}(p_3)]\}. \quad (\text{B2})$$

where $u_{1\dots 4}$ and $v_{1\dots 4}$ denote the external legs of the particles and antiparticles in Eq. (B1); $p_{1\dots 4}$ are the corresponding momenta, $s_{1\dots 4}$ are the corresponding spins. The factors of 2 in front of iG_a arise because there are four different ways of assigning initial or final states to the four ν 's in each operator and two of them have the same amplitude. The minus sign in the second row comes from exchanging fermion lines.

When computing $|\mathcal{M}_{(a)}|^2$, we sum over the spins of all the initial and final states

$$|\mathcal{M}|^2 = \sum_{s_1 s_3} \sum_{s_2 s_4} |\mathcal{M}^{s_1 s_2 s_3 s_4}|^2. \quad (\text{B3})$$

Note that for unpolarized scattering, typically there are factors of 1/2 in the spin summation. Here we are working on polarized scattering but the spins are still summed over so that one can apply the trace technology. The difference is that here we do not have factors of 1/2 in the summation, provided that the amplitude in Eq. (B2) automatically vanishes if the spins do not match the projectors P_L and P_R in Eq. (B2).

If fully expanded, Eq. (B2) contains four terms and hence Eq. (B3) contains 16 terms. The 16 terms can be converted to either one trace of Dirac matrices, e.g.,

$$\begin{aligned} & [\bar{v}_2 P_R \Gamma^a P_R u_1] [\bar{u}_4 P_R \Gamma^a P_R v_3] [\bar{u}_1 P_L \Gamma^b P_L u_4] [\bar{v}_3 P_L \Gamma^b P_L v_2] \\ & \rightarrow \text{tr} \left[P_R \Gamma^a P_R u_1 \bar{u}_1 P_L \Gamma^b P_L u_4 \bar{u}_4 P_R \Gamma^a P_R v_3 \bar{v}_3 P_L \Gamma^b P_L v_2 \bar{v}_2 \right], \end{aligned} \quad (\text{B4})$$

or two traces of two separate set of Dirac matrices, e.g.,

$$\begin{aligned} & [\bar{v}_2 P_R \Gamma^a P_R u_1] [\bar{u}_4 P_R \Gamma^a P_R v_3] [\bar{u}_1 P_L \Gamma^b P_L v_2] [\bar{v}_3 P_L \Gamma^b P_L u_4] \\ & \rightarrow \text{tr} \left[P_R \Gamma^a P_R u_1 \bar{u}_1 P_L \Gamma^b P_L v_2 \bar{v}_2 \right] \text{tr} \left[P_R \Gamma^a P_R v_3 \bar{v}_3 P_L \Gamma^b P_L u_4 \bar{u}_4 \right]. \end{aligned} \quad (\text{B5})$$

Note that Γ^a and Γ^b should have different Lorentz indices even if $a = b$.

With the aforementioned details, it is straightforward to compute $|\mathcal{M}|^2$:

$$|\mathcal{M}|^2 = 16 |G_S - 12G_T|^2 (p_1 \cdot p_3)(p_2 \cdot p_4). \quad (\text{B6})$$

Now using crossing symmetry we can quickly obtain $|\mathcal{M}|^2$ for

$$\nu_R(p_1) + \nu_R(p_2) \rightarrow \nu_L(p_3) + \nu_L(p_4) \quad (\text{B7})$$

by replacing $p_2 \rightarrow -p_3$ and $p_3 \rightarrow -p_2$ in Eq. (B6):

$$|\mathcal{M}|^2 = 16 |G_S - 12G_T|^2 (p_1 \cdot p_2)(p_3 \cdot p_4). \quad (\text{B8})$$

Next, let us consider the process

$$\nu_R(p_1) + \bar{\nu}_L(p_2) \rightarrow \nu_R(p_3) + \bar{\nu}_L(p_4), \quad (\text{B9})$$

which can only be generated by \tilde{G}_S and G_V . The amplitude is simpler compared to the previous case because for each operator there is only one way of assigning the initial/final states to the 4 ν 's in the operator:

$$i\mathcal{M}^{s_1 s_2 s_3 s_4} = i\tilde{G}_S [\bar{v}_2^{s_2}(p_2)P_R P_R u_1^{s_1}(p_1)] [\bar{u}_3^{s_3}(p_3)P_L P_L v_4^{s_4}(p_4)] \\ - iG_V [\bar{v}_2^{s_2}(p_2)P_R \gamma^\mu P_L v_4^{s_4}(p_4)] [\bar{u}_3^{s_3}(p_3)P_L \gamma_\mu P_R u_1^{s_1}(p_1)].$$

Following a similar procedure, we obtain

$$|\mathcal{M}|^2 = 4|\tilde{G}_S - 2G_V|^2(p_1 \cdot p_2)(p_3 \cdot p_4). \quad (\text{B10})$$

Again, using crossing symmetry, we can quickly obtain $|\mathcal{M}|^2$ for

$$\nu_R(p_1) + \bar{\nu}_R(p_2) \rightarrow \nu_L(p_3) + \bar{\nu}_L(p_4) \quad (\text{B11})$$

by replacing $p_2 \rightarrow -p_3$ and $p_3 \rightarrow -p_2$ in Eq. (B10):

$$|\mathcal{M}|^2 = 4|\tilde{G}_S - 2G_V|^2(p_1 \cdot p_3)(p_2 \cdot p_4). \quad (\text{B12})$$

Finally, for the process

$$\nu_R(p_1) + \nu_L(p_2) \rightarrow \nu_R(p_3) + \nu_L(p_4), \quad (\text{B13})$$

we replace $p_2 \rightarrow -p_4$ and $p_4 \rightarrow -p_2$ in Eq. (B10) and obtain:

$$|\mathcal{M}|^2 = 4|\tilde{G}_S - 2G_V|^2(p_1 \cdot p_4)(p_3 \cdot p_2). \quad (\text{B14})$$

Appendix C: Calculation of collision terms

In this appendix we present the calculation of collision terms using the technique developed in Appendix A of Ref. [38]. To make the calculation applicable to both Eqs. (A20) and (A21), we focus on the following integral

$$C \equiv - \int d\Pi_1 d\Pi_2 d\Pi_3 d\Pi_4 (2\pi)^4 \delta^4(p_1 + p_2 - p_3 - p_4) u(E_1) F |\mathcal{M}|^2, \quad (\text{C1})$$

where $d\Pi_i \equiv \frac{1}{(2\pi)^3} \frac{d^3\mathbf{p}_i}{2E_i}$, $u(E_1)$ is a general function of E_1 , and F takes F_{FD} for Fermi-Dirac statistics or F_{MB} for Maxwell-Boltzmann statistics, with F_{FD} and F_{MB} given as follows:

$$F_{\text{FD}} = f_1 f_2 (1 - f_3)(1 - f_4) - f_3 f_4 (1 - f_1)(1 - f_2), \quad f_i = \frac{1}{\exp(E_i/T_i) + 1}, \quad (\text{C2})$$

$$F_{\text{MB}} = f_1 f_2 - f_3 f_4, \quad f_i = \frac{1}{\exp(E_i/T_i)}. \quad (\text{C3})$$

Here T_i is the temperature of the i -th particle. The matrix element squared $|\mathcal{M}|^2$ is in our work given as one of three different combination of 4-vector products, see Tab. I. We write it here in general as

$$|\mathcal{M}|^2 = G_1(p_1 \cdot p_2)(p_3 \cdot p_4) + G_2(p_1 \cdot p_3)(p_2 \cdot p_4) + G_3(p_1 \cdot p_4)(p_2 \cdot p_3), \quad (\text{C4})$$

where G_1 , G_2 , and G_3 are constants.

When Eq. (C1) is applied to the collision term of number density or energy density, i.e. $C^{(n)}$ in Eq. (A20) or $C^{(\rho)}$ in Eq. (A21), we set $u(E_1) = 1$ or $u(E_1) = E_1$, respectively.

Using the identity

$$\delta^3(\mathbf{p}_1 + \mathbf{p}_2 - \mathbf{p}_3 - \mathbf{p}_4) = \int e^{i(\mathbf{p}_1 + \mathbf{p}_2 - \mathbf{p}_3 - \mathbf{p}_4) \cdot \boldsymbol{\lambda}} \frac{d^3 \boldsymbol{\lambda}}{(2\pi)^3}, \quad (\text{C5})$$

we can split Eq. (C1) into two integrals:

$$C = -\frac{1}{128\pi^5} \int \delta(E_1 + E_2 - E_3 - E_4) u(E_1) F D(p_1, p_2, p_3, p_4) \frac{p_1 dp_1}{E_1} \frac{p_2 dp_2}{E_2} \frac{p_3 dp_3}{E_3} \frac{p_4 dp_4}{E_4}, \quad (\text{C6})$$

$$D = \frac{p_1 p_2 p_3 p_4}{256\pi^6} \int d\Omega_\lambda \int_0^\infty \lambda^2 d\lambda \int d\Omega_1 e^{i\mathbf{p}_1 \cdot \boldsymbol{\lambda}} \int d\Omega_2 e^{i\mathbf{p}_2 \cdot \boldsymbol{\lambda}} \int d\Omega_3 e^{-i\mathbf{p}_3 \cdot \boldsymbol{\lambda}} \int d\Omega_4 e^{-i\mathbf{p}_4 \cdot \boldsymbol{\lambda}} |\mathcal{M}|^2, \quad (\text{C7})$$

where we have used spherical coordinates: $d^3 \mathbf{p}_i = p_i^2 dp_i d\Omega_i$ and $d^3 \boldsymbol{\lambda} = \lambda^2 d\lambda d\Omega_\lambda$. The integral D can be analytically calculated given the general form of $|\mathcal{M}|^2$ in Eq. (C4), as we shall work out below.

In a Cartesian coordinate system with $\boldsymbol{\lambda}$ set as the z -axis, we parameterize \mathbf{p}_i as

$$\mathbf{p}_i = p_i (\sin \theta_i \cos \varphi_i, \sin \theta_i \sin \varphi_i, \cos \theta_i), \quad (\text{C8})$$

so that

$$\mathbf{p}_i \cdot \mathbf{p}_j = p_i p_j [\sin \theta_i \sin \theta_j \cos(\varphi_i - \varphi_j) + \cos \theta_i \cos \theta_j], \quad (\text{C9})$$

and

$$d\Omega_i e^{i\mathbf{p}_i \cdot \boldsymbol{\lambda}} = d \cos \theta_i d\varphi_i e^{i \cos \theta_i p_i \lambda}. \quad (\text{C10})$$

For each term in Eq. (C4), it is straightforward to integrate out φ_i and θ_i . Taking $|\mathcal{M}|^2 \propto (p_1 \cdot p_2)(p_3 \cdot p_4)$ for example, we have

$$\begin{aligned} & \int d\Omega_1 e^{i\mathbf{p}_1 \cdot \boldsymbol{\lambda}} \int d\Omega_2 e^{i\mathbf{p}_2 \cdot \boldsymbol{\lambda}} \int d\Omega_3 e^{-i\mathbf{p}_3 \cdot \boldsymbol{\lambda}} \int d\Omega_4 e^{-i\mathbf{p}_4 \cdot \boldsymbol{\lambda}} (p_1 \cdot p_2)(p_3 \cdot p_4) \\ &= \int dc_1 d\varphi_1 e^{ic_1 p_1 \lambda} dc_2 d\varphi_2 e^{ic_2 p_2 \lambda} [E_1 E_2 - p_1 p_2 s_1 s_2 \cos(\varphi_1 - \varphi_2) - p_1 p_2 c_1 c_2] \\ & \quad \times \{1 \rightarrow 3, 2 \rightarrow 4, p_1 \rightarrow -p_3, p_2 \rightarrow -p_4\} \\ &= \frac{16\pi^2}{\lambda^2 p_1 p_2} \left[E_1 E_2 S_1 S_2 + p_1 p_2 \left(C_1 - \frac{S_1}{\lambda p_1} \right) \left(C_2 - \frac{S_2}{\lambda p_2} \right) \right] \\ & \quad \times \{1 \rightarrow 3, 2 \rightarrow 4, p_1 \rightarrow -p_3, p_2 \rightarrow -p_4\}, \end{aligned} \quad (\text{C11})$$

where $(c_i, s_i) \equiv (\cos \theta_i, \sin \theta_i)$ and

$$(C_i, S_i) \equiv (\cos \lambda p_i, \sin \lambda p_i). \quad (\text{C12})$$

Applying the above result to Eq. (C7), we obtain

$$\begin{aligned} D^{(1,2)(3,4)} &= \frac{4G_1}{\pi} \int_0^\infty \lambda^{-2} d\lambda \left[E_1 E_2 S_1 S_2 + p_1 p_2 \left(C_1 - \frac{S_1}{\lambda p_1} \right) \left(C_2 - \frac{S_2}{\lambda p_2} \right) \right] \\ & \quad \times \left[E_3 E_4 S_3 S_4 + p_3 p_4 \left(C_3 - \frac{S_3}{\lambda p_3} \right) \left(C_4 - \frac{S_4}{\lambda p_4} \right) \right]. \end{aligned} \quad (\text{C13})$$

Here the superscript $(1 \cdot 2)(3 \cdot 4)$ is to remind us that so far we have only considered the $G_1(p_1 \cdot p_2)(p_3 \cdot p_4)$ term. Eq. (C13) can be decomposed as

$$D^{(1 \cdot 2)(3 \cdot 4)} = G_1 E_1 E_2 E_3 E_4 D_{SS} + G_1 E_1 E_2 p_3 p_4 D_{SC} \\ + G_1 p_1 p_2 E_3 E_4 D_{CS} + G_1 p_1 p_2 p_3 p_4 D_{CC}, \quad (\text{C14})$$

where

$$D_{SS} = \frac{4}{\pi} \int_0^\infty \frac{d\lambda}{\lambda^2} S_1 S_2 S_3 S_4, \quad (\text{C15})$$

$$D_{SC} = \frac{4}{\pi} \int_0^\infty \frac{d\lambda}{\lambda^2} S_1 S_2 \left(C_3 - \frac{S_3}{\lambda p_3} \right) \left(C_4 - \frac{S_4}{\lambda p_4} \right), \quad (\text{C16})$$

$$D_{CS} = \frac{4}{\pi} \int_0^\infty \frac{d\lambda}{\lambda^2} S_3 S_4 \left(C_1 - \frac{S_1}{\lambda p_1} \right) \left(C_2 - \frac{S_2}{\lambda p_2} \right), \quad (\text{C17})$$

$$D_{CC} = \frac{4}{\pi} \int_0^\infty \frac{d\lambda}{\lambda^2} \left(C_1 - \frac{S_1}{\lambda p_1} \right) \left(C_2 - \frac{S_2}{\lambda p_2} \right) \left(C_3 - \frac{S_3}{\lambda p_3} \right) \left(C_4 - \frac{S_4}{\lambda p_4} \right). \quad (\text{C18})$$

The integration of λ in Eqs. (C15)-(C18) seems straightforward as one can express the trigonometric functions to exponential functions and then convert the integrals to Euler's gamma functions. It is worth mentioning, however, that one should handle the branch cut singularities in the gamma functions carefully. Taking Eq. (C15) for example, we may meet integrals of $\int \frac{d\lambda}{\lambda^2} \exp(i\lambda p)$, where p can be $p_1 + p_2 + p_3 + p_4$, $p_1 - p_2 + p_3 - p_4$, $p_1 + p_2 - p_3 - p_4$, etc. This integral is divergent but the divergence is expected to be canceled out in Eq. (C15). One can regulate the integral by limiting it in $\lambda \in [\epsilon, \infty)$ with $\epsilon > 0$. The result depends on whether $p > 0$ or < 0 :

$$\lim_{\epsilon \rightarrow 0^+} \int_\epsilon^\infty \frac{d\lambda}{\lambda^2} e^{i\lambda p} = \begin{cases} \frac{1}{\epsilon} - \frac{\pi p}{2} - ip [\log(p\epsilon) + \gamma_E - 1] & \text{for } p > 0 \\ \frac{1}{\epsilon} + \frac{\pi p}{2} - ip [\log(-p\epsilon) + \gamma_E - 1] & \text{for } p < 0 \end{cases}, \quad (\text{C19})$$

where $\gamma_E \approx 0.577216$ is Euler's constant. As a consequence, the result of D_{SS} depends on whether $p_1 - p_2 + p_3 - p_4 > 0$, $p_1 + p_2 - p_3 - p_4 > 0$, $p_1 - p_2 - p_3 + p_4 > 0$, etc.

With the above details being noted, we present the results of D_{SS} , D_{SC} , D_{CS} and D_{CC} :

$$D_{SS} = \begin{cases} \frac{1}{2} (-p_1 + p_2 + p_3 + p_4) & \text{(condition A)} \\ p_4 & \text{(condition B)} \\ \frac{1}{2} (p_1 + p_2 - p_3 + p_4) & \text{(condition C)} \\ p_2 & \text{(condition D)} \end{cases}, \quad (\text{C20})$$

$$D_{SC} = \frac{1}{p_3 p_4} \times \begin{cases} \frac{(p_1 - p_2)^3 - 3(p_3^2 + p_4^2)(p_1 - p_2) + 2(p_3^3 + p_4^3)}{12} & \text{(condition A)} \\ \frac{p_4^3}{3} & \text{(condition B)} \\ \frac{-(p_1 + p_2)^3 + 3(p_3^2 + p_4^2)(p_1 + p_2) - 2(p_3^3 - p_4^3)}{12} & \text{(condition C)} \\ -\frac{1}{6} p_2 (3p_1^2 + p_2^2 - 3(p_3^2 + p_4^2)) & \text{(condition D)} \end{cases}, \quad (\text{C21})$$

$$D_{CS} = D_{SC}|_{p_1 \leftrightarrow p_3, p_2 \leftrightarrow p_4}, \quad (\text{C22})$$

$$D_{CC} = \frac{1}{p_1 p_2 p_3 p_4} \times \begin{cases} D_{CC}^{(A)} & \text{(condition A)} \\ \frac{1}{30} (5(p_1^2 + p_2^2 + p_3^2) p_4^3 - p_4^5) & \text{(condition B)} \\ D_{CC}^{(C)} & \text{(condition C)} \\ \frac{1}{30} p_2^3 (5p_1^2 - p_2^2 + 5(p_3^2 + p_4^2)) & \text{(condition D)} \end{cases}, \quad (\text{C23})$$

$$\begin{aligned}
D_{CC}^{(A)} \equiv & \frac{p_1^5}{60} - \frac{1}{12}p_2^2p_1^3 - \frac{1}{12}p_3^2p_1^3 - \frac{1}{12}p_4^2p_1^3 + \frac{1}{12}p_3^3p_1^2 + \frac{1}{12}p_3^3p_1^2 + \frac{1}{12}p_4^3p_1^2 + \frac{1}{12}p_2^2p_3^3 \\
& + \frac{1}{12}p_2^2p_4^3 + \frac{1}{12}p_3^2p_4^3 + \frac{1}{12}p_2^3p_3^2 + \frac{1}{12}p_2^3p_4^2 + \frac{1}{12}p_3^3p_4^2 - \frac{p_2^5}{60} - \frac{p_3^5}{60} - \frac{p_4^5}{60}, \tag{C24}
\end{aligned}$$

$$D_{CC}^{(C)} = D_{CC}^{(A)} \Big|_{p_1 \leftrightarrow p_3, p_2 \leftrightarrow p_4}.$$

Here we need to distinguish four conditions:

$$\text{(condition A)} : p_1 + p_2 \geq p_3 + p_4 \wedge p_1 + p_4 \geq p_2 + p_3 \wedge p_1 \geq p_2 \wedge p_3 \geq p_4, \tag{C25}$$

$$\text{(condition B)} : p_1 + p_2 \geq p_3 + p_4 \wedge p_1 + p_4 < p_2 + p_3 \wedge p_1 \geq p_2 \wedge p_3 \geq p_4, \tag{C26}$$

$$\text{(condition C)} : p_1 + p_2 < p_3 + p_4 \wedge p_1 + p_4 < p_2 + p_3 \wedge p_1 \geq p_2 \wedge p_3 \geq p_4, \tag{C27}$$

$$\text{(condition D)} : p_1 + p_2 < p_3 + p_4 \wedge p_1 + p_4 \geq p_2 + p_3 \wedge p_1 \geq p_2 \wedge p_3 \geq p_4. \tag{C28}$$

Note that here we only present results for $p_1 \geq p_2 \wedge p_3 \geq p_4$. Since Eqs. (C15)-(C18) are symmetric under $1 \leftrightarrow 2$ and (or) $3 \leftrightarrow 4$, results for other possibilities such as $p_1 \geq p_2 \wedge p_3 < p_4$, $p_1 < p_2 \wedge p_3 \geq p_4$, and $p_1 < p_2 \wedge p_3 < p_4$ can be obtained by exchanging $1 \leftrightarrow 2$ and (or) $3 \leftrightarrow 4$.

So far we have not made any assumptions about the particle masses, so the above calculations apply to both massless and massive particles.

Next, we proceed with the integral in Eq. (C6). Taking the massless assumption $E_i = p_i$, Eq. (C6) can be written as

$$C^{(1\cdot2)(3\cdot4)} = -\frac{G_1}{128\pi^5} \int u(p_1) F p_1 p_2 p_3 p_4 (D_{SS} + D_{SC} + D_{CS} + D_{CC}) dp_1 dp_3 dp_4, \tag{C29}$$

where p_2 should be replaced by $p_3 + p_4 - p_1$. Using the D -functions in Eqs. (C20)-(C23) and $F = F_{\text{MB}}$ in Eq. (C3), we obtain

$$C^{(1\cdot2)(3\cdot4)} = \frac{G_1}{8\pi^5} \times \begin{cases} 3T_3^4 T_4^4 - 3T_1^4 T_2^4 & \text{for number density} \\ 6T_3^4 T_4^4 (T_3 + T_4) - 12T_1^5 T_2^4 & \text{for energy density} \end{cases}. \tag{C30}$$

Here the superscript $(1\cdot2)(3\cdot4)$ reminds us that the result is only for the $G_1(p_1 \cdot p_2)(p_3 \cdot p_4)$ term. For other two terms in $|\mathcal{M}|^2$, namely $G_2(p_1 \cdot p_3)(p_2 \cdot p_4)$ and $G_3(p_1 \cdot p_4)(p_2 \cdot p_3)$, the calculation is similar and we find that Eq. (C29) should be modified to:

$$C^{(1\cdot3)(2\cdot4)} = -\frac{G_2}{128\pi^5} \int u(p_1) F p_1 p_2 p_3 p_4 [D_{SS} - D_{SC} - D_{CS} + D_{CC}]_{p_2 \leftrightarrow p_3} dp_1 dp_3 dp_4, \tag{C31}$$

and

$$C^{(1\cdot4)(2\cdot3)} = -\frac{G_3}{128\pi^5} \int u(p_1) F p_1 p_2 p_3 p_4 [D_{SS} - D_{SC} - D_{CS} + D_{CC}]_{p_2 \leftrightarrow p_4} dp_1 dp_3 dp_4. \tag{C32}$$

Note that the minus signs before D_{SC} and D_{CS} originate from the minus signs in $e^{-i\mathbf{p}_3 \cdot \boldsymbol{\lambda}}$ and $e^{-i\mathbf{p}_4 \cdot \boldsymbol{\lambda}}$. The results of Eqs. (C31) and (C32) read:

$$C^{(1\cdot3)(2\cdot4)} = \frac{G_2}{8\pi^5} \times \begin{cases} T_3^4 T_4^4 - T_1^4 T_2^4 & \text{for number density} \\ T_3^4 T_4^4 (T_3 + 3T_4) - 4T_1^5 T_2^4 & \text{for energy density} \end{cases}, \tag{C33}$$

$$C^{(1\cdot4)(2\cdot3)} = \frac{G_3}{8\pi^5} \times \begin{cases} T_3^4 T_4^4 - T_1^4 T_2^4 & \text{for number density} \\ T_3^4 T_4^4 (3T_3 + T_4) - 4T_1^5 T_2^4 & \text{for energy density} \end{cases}. \tag{C34}$$

Table III. Collision terms for energy density ($C^{(\rho)}$) and for number density ($C^{(n)}$). The analytical expressions for $C_{\text{MB}}^{(\rho)}$ and $C_{\text{MB}}^{(n)}$ have been computed assuming Maxwell-Boltzmann statistics. For Fermi-Dirac statistics, one should multiply C_{MB} by the numerical factors $1 - \delta_{\text{FD}}$ to include the difference.

$ M^2 $	$T_1 = T_2, T_3 = T_4$ (annihilation)				$T_1 = T_3, T_2 = T_4$ (scattering)		
	$C_{\text{MB}}^{(\rho)}$	$1 - \delta_{\text{FD}}^{(\rho)}$	$C_{\text{MB}}^{(n)}$	$1 - \delta_{\text{FD}}^{(n)}$	$C_{\text{MB}}^{(\rho)}$	$1 - \delta_{\text{FD}}^{(\rho)}$	$C_{\text{MB}}^{(n)}$
$(p_1 \cdot p_2)(p_3 \cdot p_4)$	$\frac{3(T_3^9 - T_1^9)}{2\pi^5}$	0.8840	$\frac{3(T_3^8 - T_1^8)}{8\pi^5}$	0.8521	$\frac{3T_2^4 T_1^4 (T_2 - T_1)}{4\pi^5}$	0.8249	0
$(p_1 \cdot p_3)(p_2 \cdot p_4)$	$\frac{T_3^9 - T_1^9}{2\pi^5}$	0.8841	$\frac{T_3^8 - T_1^8}{8\pi^5}$	0.8523	$\frac{3T_2^4 T_1^4 (T_2 - T_1)}{8\pi^5}$	0.8118	0
$(p_1 \cdot p_4)(p_2 \cdot p_3)$	$\frac{T_3^9 - T_1^9}{2\pi^5}$	0.8841	$\frac{T_3^8 - T_1^8}{8\pi^5}$	0.8523	$\frac{T_2^4 T_1^4 (T_2 - T_1)}{8\pi^5}$	0.8518	0

In practical use, we often have: (i) $T_1 = T_2, T_3 = T_4$, (ii) $T_1 = T_3, T_2 = T_4$, or (iii) $T_1 = T_4, T_2 = T_3$. Case (i) appears when computing the collision term of an annihilation process, and the last two cases apply to ν_R scattering with ν_L . In Tab. III, we summarize the results of the collision terms for cases (i) and (ii). For case (iii), the result can be obtained from (ii) with $T_3 \leftrightarrow T_4$ and $p_3 \leftrightarrow p_4$.

The analytical results in Eqs. (C30), (C33), and (C34) are only for Maxwell-Boltzmann statistics. For Fermi-Dirac statistics, we numerically evaluate Eqs. (C29), (C31), and (C32) with $F = F_{\text{FD}}$ given in Eq. (C2). Then we compute the ratio between the Fermi-Dirac result (C_{FD}) and the Maxwell-Boltzmann one (C_{MB}):

$$1 - \delta_{\text{FD}} \equiv \frac{C_{\text{FD}}}{C_{\text{MB}}}. \quad (\text{C35})$$

The ratio is temperature-dependent. But for the aforementioned three cases (i, ii, iii), $1 - \delta_{\text{FD}}$ only depends on $\Delta T/T_1$ where ΔT is the difference between T_1 and the other different temperature. When $\Delta T/T_1$ is large, the collision term is not important because it implies that ν_R has decoupled. So we are mainly interested in the value of $1 - \delta_{\text{FD}}$ when $\Delta T/T_1 \ll 1$ and we have found that in this case $1 - \delta_{\text{FD}}$ is insensitive to $\Delta T/T_1$. We compute the values of $1 - \delta_{\text{FD}}$ in the limit $\Delta T/T_1 \rightarrow 0$, and the results are summarized in Tab. III.

-
- [1] M. J. Dolinski, A. W. Poon, and W. Rodejohann, *Neutrinoless Double-Beta Decay: Status and Prospects*, *Ann. Rev. Nucl. Part. Sci.* **69** (2019) 219–251, [[1902.04097](#)].
 - [2] Z.-z. Xing, *Flavor structures of charged fermions and massive neutrinos*, [[1909.09610](#)].
 - [3] A. D. Dolgov, *Neutrinos in cosmology*, *Phys. Rept.* **370** (2002) 333–535, [[hep-ph/0202122](#)].
 - [4] E. Masso and R. Toldra, *Constraints on neutrino-neutrino interactions from primordial nucleosynthesis*, *Phys. Lett.* **B333** (1994) 132–134, [[hep-ph/9404339](#)].
 - [5] **Planck Collaboration**, Y. Akrami *et al.*, *Planck 2018 results. I. Overview and the cosmological legacy of Planck*, [[1807.06205](#)].
 - [6] **Planck Collaboration**, N. Aghanim *et al.*, *Planck 2018 results. VI. Cosmological parameters*, [[1807.06209](#)].
 - [7] G. Mangano, G. Miele, S. Pastor, T. Pinto, O. Pisanti, and P. D. Serpico, *Relic neutrino decoupling including flavor oscillations*, *Nucl. Phys. B* **729** (2005) 221–234, [[hep-ph/0506164](#)].
 - [8] E. Grohs, G. M. Fuller, C. T. Kishimoto, M. W. Paris, and A. Vlasenko, *Neutrino energy transport in weak decoupling and big bang nucleosynthesis*, *Phys. Rev. D* **93** (2016), no. 8 083522, [[1512.02205](#)].
 - [9] P. F. de Salas and S. Pastor, *Relic neutrino decoupling with flavour oscillations revisited*, *JCAP* **07** (2016) 051, [[1606.06986](#)].
 - [10] **CMB-S4 Collaboration**, K. N. Abazajian *et al.*, *CMB-S4 Science Book, First Edition*, [[1610.02743](#)].
 - [11] K. Abazajian *et al.*, *CMB-S4 Science Case, Reference Design, and Project Plan*, [[1907.04473](#)].

- [12] K. N. Abazajian and J. Heeck, *Observing Dirac neutrinos in the cosmic microwave background*, *Phys. Rev. D* **100** (2019) 075027, [[1908.03286](#)].
- [13] S. Davidson, C. Pena-Garay, N. Rius, and A. Santamaria, *Present and future bounds on nonstandard neutrino interactions*, *JHEP* **03** (2003) 011, [[hep-ph/0302093](#)].
- [14] T. Ohlsson, *Status of non-standard neutrino interactions*, *Rept. Prog. Phys.* **76** (2013) 044201, [[1209.2710](#)].
- [15] Y. Farzan and M. Tortola, *Neutrino oscillations and Non-Standard Interactions*, *Front.in Phys.* **6** (2018) 10, [[1710.09360](#)].
- [16] P. Bhupal Dev *et al.*, *Neutrino Non-Standard Interactions: A Status Report*, *SciPost Phys. Proc.* **2** (2019) 001, [[1907.00991](#)].
- [17] C. Boehm, M. J. Dolan, and C. McCabe, *Increasing N_{eff} with particles in thermal equilibrium with neutrinos*, *JCAP* **1212** (2012) 027, [[1207.0497](#)].
- [18] A. Kamada and H.-B. Yu, *Coherent Propagation of PeV Neutrinos and the Dip in the Neutrino Spectrum at IceCube*, *Phys. Rev. D* **92** (2015), no. 11 113004, [[1504.00711](#)].
- [19] G.-y. Huang, T. Ohlsson, and S. Zhou, *Observational Constraints on Secret Neutrino Interactions from Big Bang Nucleosynthesis*, *Phys. Rev. D* **97** (2018), no. 7 075009, [[1712.04792](#)].
- [20] A. Fradette, M. Pospelov, J. Pradler, and A. Ritz, *Cosmological beam dump: constraints on dark scalars mixed with the Higgs boson*, *Phys. Rev. D* **99** (2019), no. 7 075004, [[1812.07585](#)].
- [21] M. Escudero, *Neutrino decoupling beyond the Standard Model: CMB constraints on the Dark Matter mass with a fast and precise N_{eff} evaluation*, *JCAP* **1902** (2019) 007, [[1812.05605](#)].
- [22] M. Escudero Abenza, *Precision Early Universe Thermodynamics made simple: N_{eff} and Neutrino Decoupling in the Standard Model and beyond*, [2001.04466](#).
- [23] P. F. Depta, M. Hufnagel, K. Schmidt-Hoberg, and S. Wild, *BBN constraints on the annihilation of MeV-scale dark matter*, *JCAP* **1904** (2019) 029, [[1901.06944](#)].
- [24] M. Lindner, W. Rodejohann, and X.-J. Xu, *Coherent Neutrino-Nucleus Scattering and new Neutrino Interactions*, *JHEP* **03** (2017) 097, [[1612.04150](#)].
- [25] W. Rodejohann, X.-J. Xu, and C. E. Yaguna, *Distinguishing between Dirac and Majorana neutrinos in the presence of general interactions*, *JHEP* **05** (2017) 024, [[1702.05721](#)].
- [26] D. Papoulias and T. Kosmas, *COHERENT constraints to conventional and exotic neutrino physics*, *Phys. Rev. D* **97** (2018), no. 3 033003, [[1711.09773](#)].
- [27] D. Aristizabal Sierra, V. De Romeri, and N. Rojas, *COHERENT analysis of neutrino generalized interactions*, *Phys. Rev. D* **98** (2018) 075018, [[1806.07424](#)].
- [28] C. Boehm, D. Cerdeno, P. Machado, A. Olivares-Del Campo, E. Perdomo, and E. Reid, *How high is the neutrino floor?*, *JCAP* **01** (2019) 043, [[1809.06385](#)].
- [29] I. Bischer and W. Rodejohann, *General Neutrino Interactions at the DUNE Near Detector*, *Phys. Rev. D* **99** (2019), no. 3 036006, [[1810.02220](#)].
- [30] X.-J. Xu, *Tensor and scalar interactions of neutrinos may lead to observable neutrino magnetic moments*, *Phys. Rev. D* **99** (2019), no. 7 075003, [[1901.00482](#)].
- [31] P. D. Bolton and F. F. Deppisch, *Probing nonstandard lepton number violating interactions in neutrino oscillations*, *Phys. Rev. D* **99** (2019), no. 11 115011, [[1903.06557](#)].
- [32] W. Chao, J.-G. Jiang, X. Wang, and X.-Y. Zhang, *Direct Detections of Dark Matter in the Presence of Non-standard Neutrino Interactions*, *JCAP* **08** (2019) 010, [[1904.11214](#)].
- [33] I. Bischer and W. Rodejohann, *General neutrino interactions from an effective field theory perspective*, *Nucl. Phys. B* **947** (2019) 114746, [[1905.08699](#)].
- [34] A. N. Khan, W. Rodejohann, and X.-J. Xu, *Borexino and general neutrino interactions*, *Phys. Rev. D* **101** (2020), no. 5 055047, [[1906.12102](#)].
- [35] P. D. Bolton, F. F. Deppisch, and C. Hati, *Probing New Physics with Long-Range Neutrino Interactions: An Effective Field Theory Approach*, [2004.08328](#).
- [36] T. Han, J. Liao, H. Liu, and D. Marfatia, *Scalar and tensor neutrino interactions*, [2004.13869](#).
- [37] S. Hannestad and J. Madsen, *Neutrino decoupling in the early universe*, *Phys. Rev. D* **52** (1995) 1764–1769, [[astro-ph/9506015](#)].
- [38] A. Dolgov, S. Hansen, and D. Semikoz, *Nonequilibrium corrections to the spectra of massless neutrinos in the early universe*, *Nucl. Phys. B* **503** (1997) 426–444, [[hep-ph/9703315](#)].
- [39] L. Husdal, *On Effective Degrees of Freedom in the Early Universe*, *Galaxies* **4** (2016), no. 4 78, [[1609.04979](#)].

- [40] **SPT-3G Collaboration**, B. Benson *et al.*, *SPT-3G: A Next-Generation Cosmic Microwave Background Polarization Experiment on the South Pole Telescope*, *Proc. SPIE Int. Soc. Opt. Eng.* **9153** (2014) 91531P, [[1407.2973](#)].
- [41] **Simons Observatory Collaboration**, M. H. Abitbol *et al.*, *The Simons Observatory: Astro2020 Decadal Project Whitepaper*, *Bull. Am. Astron. Soc.* **51** (2019) 147, [[1907.08284](#)].
- [42] E. W. Kolb and M. S. Turner, *The Early Universe*, Addison-Wesley Publishing Company, 1990, USA.